textiles

MDPI

Article

Influence of the Structure of 3D Woven Fabrics on Radiation Heat Resistance and Thermophysiology Properties

Ana Kiš [1,*] and Stana Kovačević [2]

[1] Vertiv Croatia d.o.o., Oreškovićeva 6n/2, 10000 Zagreb, Croatia
[2] Department of Textile Design and Management, Faculty and Textile Technology, University of Zagreb, Prilaz baruna Filipovića 28a, 10000 Zagreb, Croatia; stana.kovacevic@ttf.unizg.hr
* Correspondence: akis@ttf.hr

Abstract: The goal of this study was to investigate the influence of structural and constructional parameters of 3D fabric on two of the most significant properties of fabrics for thermal protection—resistance to radiation heat and thermophysiological properties. Today's textile materials provide high thermal protection, but they display poor thermophysiological properties in extreme conditions. Six samples of 3D fabrics were developed using a laboratory weaving machine. The examined samples were made of identical warp, with a total of three different weft densities, and were woven in two different weaves. The conditions of the weaving process and construction were the same. EN ISO 6942:2022 and EN ISO 11092:2014 methods were used to determine the resistance of the samples to thermal radiation and thermophysiological properties. The results showed that the samples that contained folds in their structure with a larger volume of "trapped" air had better thermophysiological properties and better resistance to thermal radiation. The volume of air contained in the 3D structure was used as a thermal insulator and it did not have a negative effect on the thermophysiological properties. The described structure enabled the 3D fabric to have an optimal ratio of thermal protection and comfort, which is of crucial importance for fabrics used to make thermal protective clothing.

Keywords: 3D fabrics; water vapor resistance; heat resistance; resistance to radiant heat

Citation: Kiš, A.; Kovačević, S. Influence of the Structure of 3D Woven Fabrics on Radiation Heat Resistance and Thermophysiology Properties. *Textiles* **2024**, *4*, 267–283. https://doi.org/10.3390/textiles4020016

Academic Editor: Rajesh Mishra

Received: 29 March 2024
Revised: 3 June 2024
Accepted: 8 June 2024
Published: 17 June 2024

1. Introduction

Fabrics used for thermal protective clothing are generally dense, semi-permeable and/or air-tight to ensure a high level of protection for firefighters and people of similar professions [1–3]. The requirements for firefighting clothing are numerous. For example, a firefighter can spend between 8 and 16 h actively fighting outdoor fire. Therefore, in addition to protection against high temperatures and flames, there are requirements for wearing comfort (increased mobility, breathability). The two most important factors are maximizing thermal fire protection and minimizing metabolic heat stress. Ensuring thermal protection is a critical requirement to consider when creating firefighting protective clothing, as well as the comfort that the firefighter feels while enduring extreme thermal stress [4]. The effect of the thermal protective clothing depends on the heat transfer between the clothing as a reactor and the source of the fire. Thermal protective clothing tends to be heavy, stiff, and voluminous, which increases the load on a wearer. This consequently leads to metabolic heat production, which is common during highly stressful conditions to which the emergency response teams are often exposed [5]. Therefore, thermal protective clothing must perform two opposite functions: it should stop the heat from the environment flowing towards the body, while simultaneously allowing the metabolic heat to escape into the atmosphere [6]. In order for the fabric from which the thermal protective clothing is made to become an adequate protective barrier, it must be made of appropriate materials, taking into account the raw materials used, where the structural and construction parameters are crucial. Nowadays, the most commonly used fibers for making thermal protective clothes

are meta-aramid and para-aramid fibers. Both meta-aramid and para-aramid fibers have shown very high thermal stability. In addition, para-aramid fibers are characterised by high mechanical properties, which makes them useful for ballistic purposes [7].

The characteristics of the used fibers, the thickness of the fabric and the air trapped in the fabric's pore pockets determine the permeability of the thermal and vapor insulation. Many different factors have an impact on the performance of thermal protective clothing, such as environmental conditions (temperature, humidity, wind speed, etc.), the nature of the textile used (structure, weight and thickness of fabric, type of fiber, etc.), mechanism for heat transfer (convection, conductivity, thermal radiation), and the existence of moisture [8,9].

During intense activity, the human body cools down by releasing sweat and allows for sweat evaporation. Clothing must be able to wick away this moisture to maintain comfort and reduce the degradation of thermal insulation caused by moisture accumulation in a cold environment. This is why the transfer of water vapor is important in determining the breathability of fabrics by layers. Breathable fabrics allow additional heat loss by evaporating moisture through layers of clothing. If the layers of clothing are impermeable, heat and moisture accumulate between the skin and the clothing, resulting in discomfort due to the feeling of wetness and abrasion of the skin. In terms of thermophysiological comfort, the two most important parameters relate to the movement of heat and sweat from the body and can be measured in terms of thermal insulation and resistance to water vapor [10]. When the body gains heat at a faster rate than it can lose it, there is a risk of the body experiencing heat stroke.

Heat transfer through fabrics is largely related to its capillary structure and the surface characteristics of the yarn, as well as the distribution of air volume within the fabrics. This is a complex phenomenon, dependent on numerous parameters such as fabric geometry, fabric thickness [11], fabric density, yarn structure, weaving method, and number of fabric layers [12]. By interweaving the warp and weft threads at a right angle, an intermediate space or pore is created between the connecting points of two adjacent threads. Fabric with larger pores has higher porosity, i.e., higher medium permeability. The size of the pores depends primarily on the density of the fabric and the fineness of the threads. Their size also depends on the weave, surface smoothness and uniformity of the thread, raw material composition and physical–mechanical properties of the thread. The porosity property of the fabric is of great importance for technical protective fabrics [13]. The structure of the fabric affects its porosity, i.e., the amount of air it contains. Air 'trapped' in the fabric's pore pockets acts as a good heat insulator; therefore, it consequently increases the heat protection [14].

Due to the described problem, the contemporary science research is moving towards the developing and improving the added values of composites and raw materials that would accomplish the requirements which cannot be achieved with conventional fabrics that uses the concept of 3D structures. The 3D fabrics with third dimension (thickness) emphasized can be woven on classic weaving machines where two fabrics are either interwoven with individual warps, or the weft threads are created at the same time while a unique complete structure is being created simultaneously. The 3D fabrics consist of two groups of yarns, i.e., warp, weft, and interwoven warp or weft threads that periodically join the upper and lower fabrics. This is a standard process of weaving on classic weaving machines. These weaving machines are often equipped with two or three warp rollers and warps that produce different shrinkages of the fabric. In order to produce more complex fabric structures, an extensive reconstruction of the classic weaving machines is required, if not a complete design change, mostly related to the weaving system [15,16]. Several types of 3D woven structures are known, including orthogonal, corner-connected, multilayer, through-thickness and layer-by-layer structures. These structures can be produced with either a conventional or modified loom, as well as with a 3D weaving machine [17–19].

In [20], the authors analyzed the developed 3D fabrics by microscopic analysis, which are also the subject of research in this paper. The surface of 3D woven fabrics and their 3D structure was analyzed. The authors used the digital microscope Dino-Lite Edge–5 megapix AM7115MZT with a polarizing filter and a magnification of 20 times. The upper fabric

that was analyzed was the face of the fabric and was made of higher density aramid fibers. The results of the analysis showed that the upper fabric had a uniform surface. The lower fabric, made of cotton and modacrylic, was of lower density and had a wrinkled surface created by interweaving with the upper fabric. The crease on the fabric surface maintained a permanent distance between the fabrics, thus forming a pocket filled with air that was 'trapped' in a three-dimensional system. As the density of the weft increased, the folds became more frequent and denser, with less air volume. This process had an effect on the volume, thickness, and weight of the fabric. On the other hand, by reducing the density of the weft, the number of folds decreased, but such folds were filled with a larger volume of air. Also, microscopic analysis showed that the weave of the fabric had an influence on the number and size of folds. In the lower fabric of the 3D fabric in the twill weave, the folds were denser and more numerous, and in the case of the plain weave in the lower fabric, the folds were less frequent but with a larger air volume. The described structure of 3D fabrics is interesting for analyzing the influence of such a structure on thermophysiological properties and resistance to high temperatures.

2. Materials and Methods

2.1. Laboratory Weaving Machine—Fanyuan Instrument, Model DW598, China

The 3D fabric samples were made using a fully automated laboratory weaving machine (Figure 1), which is used to make fabrics from different types of yarns, equipped with two roller bases and with the following characteristics:

- Weft entry with one rigid weft bar.
- Automatic control with the CAD/CAM weaving system.
- Weft pinning device with the ability to adjust the pinning force.
- Maximum base width: 50 cm.
- Number of wefts per minute: 30–60.
- Maximum number of sheets: 20.
- Automatic, electronic weft selector.
- Number of jobs for bobbins for weft: 8.
- Device for releasing the warp.
- Automatic regulation of warp tension.
- Device for pulling fabric with the ability to regulate the weft density.
- Computer and specialized software for sample design.

Figure 1. Laboratory weaving machine—Fanyuan instrument/model DW598/Hafei Fanyuan instrument, Hefei City, China.

2.2. Samples of 3D Woven Fabrics

The supplier of yarns used in this research was Predilnica Litija, Litia, Slovenia. Six 3D fabrics were developed that consisted of the following two groups of yarns: warp, weft and interlaced threads of the warp or wefts that periodically join the upper and lower fabric to create a unique overall structure. The yarn composition of the upper and lower fabric of the warp and weft was the same for all samples, as follows: for the upper fabric, warp—95.0% M-aramid Conex NEO/weft—5% P-aramid Twaron; for the bottom fabric, base—45.0% Cotton Long Stapel Combed/weft—55% Modacrylic Sevel FRSA/L. The weave of the bottom fabric was plain weave in all samples. The weave of the upper fabric was plain weave or twill 3/1. Also, in the samples of the upper and lower fabric, the density of the weft changed, while the density of the warp remained the same in all samples. The basic parameters of the 3D fabric samples are shown in Table 1.

Table 1. Construction parameters of 3D woven samples [20].

Sample	Woven Fabric	Weave of Upper–Lower Fabric	Density of Warp–Weft (thread/cm)	Yarn Fineness (Tex)		Yarn Composition	Mass Per Unit Area (g/m^2)	Thickness (mm)
				Warp	Weft	Warp and Weft		
1pp [1]	Upper	Plain	40–35	12.5 × 2	16.7 × 2	95.0% M-aramid Conex NEO 5.0% P-aramid Twaron	356	0.63
	Lower	Plain	20–17	12.5 × 2	25	45.0% Cotton Long Stapel Combed 55.0% Modacrylic Sevel FRSA/L		
2pp	Upper	Plain	40–32	12.5 × 2	16.7 × 2	95.0% M-aramid Conex NEO 5.0% P-aramid Twaron	336	0.61
	Lower	Plain	20–16	17 × 2	25	45.0% Cotton Long Stapel Combed 55.0% Modacrylic Sevel FRSA/L		
3pp	Upper	Plain	40–30	12.5 × 2	16.7 × 2	95.0% M-aramid Conex NEO 5.0% P-aramid Twaron	303	0.59
	Lower	Plain	20–14	17 × 2	25	45.0% Cotton Long Stapel Combed 55.0% Modacrylic Sevel FRSA/L		
1tp [2]	Upper	Twill 3/1	40–35	12.5 × 2	16.7 × 2	95.0% M-aramid Conex NEO 5.0% P-aramid Twaron	316	0.61
	Lower	Plain	20–17	17 × 2	25	45.0% Cotton Long Stapel Combed 55.0% Modacrylic Sevel FRSA/L		
2tp	Upper	Twill 3/1	40–32	12.5 × 2	16.7 × 2	95.0% M-aramid Conex NEO 5.0% P-aramid Twaron	293	0.58
	Lower	Plain	20–16	17 × 2	25	45.0% Cotton Long Stapel Combed 55.0% Modacrylic Sevel FRSA/L		

Table 1. *Cont.*

Sample	Woven Fabric	Weave of Upper–Lower Fabric	Density of Warp–Weft (thread/cm)	Yarn Fineness (Tex)		Yarn Composition	Mass Per Unit Area (g/m^2)	Thickness (mm)
				Warp	Weft	Warp and Weft		
3tp	Upper	Twill 3/1	40–30	12.5 × 2	16.7 × 2	95.0% M-aramid Conex NEO 5.0% P-aramid Twaron	287	0.58
	Lower	Plain	20–14	17 × 2	25	45.0% Cotton Long Stapel Combed 55.0% Modacrylic Sevel FRSA/L		

[1] pp—plain/plain; [2] tp—twill 3/1/plain.

The cross section of the 3D fabric marked 'pp' and 'tp' is shown in Figures 2 and 3.

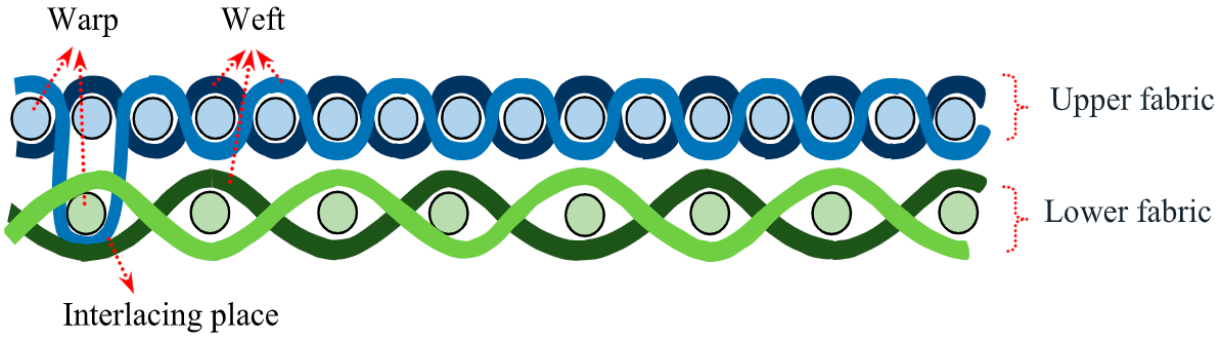

Figure 2. Section of the fabric 'pp' in the weft direction.

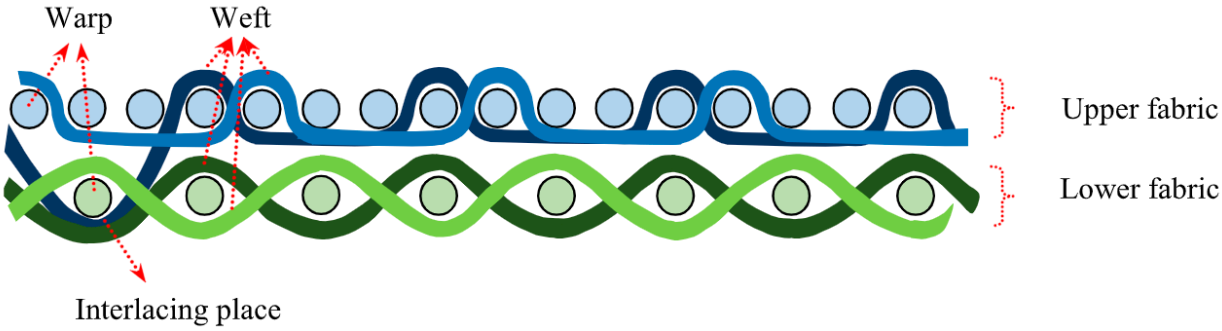

Figure 3. Section of the fabric 'tp' in the weft direction.

The structural elements and connections of the 3D fabric marked "pp" are shown in Figure 4, and the 3D fabric marked "tp" is shown in Figure 5.

Figure 6 shows microscopic images on the Digital Microscope Dino-Lite Edge-5 Megapix AM7115MZT with a polarising filter and magnification of 20×. The microscope of these characteristics is best suited to capture the cross-section of fabrics with a larger increase in the image, a larger group or the structure of the fabric could not be seen.

Figure 7 shows the cross-section of the 3D woven fabric in the plain weave with the highlighted places of the upper and lower fabric interlacing.

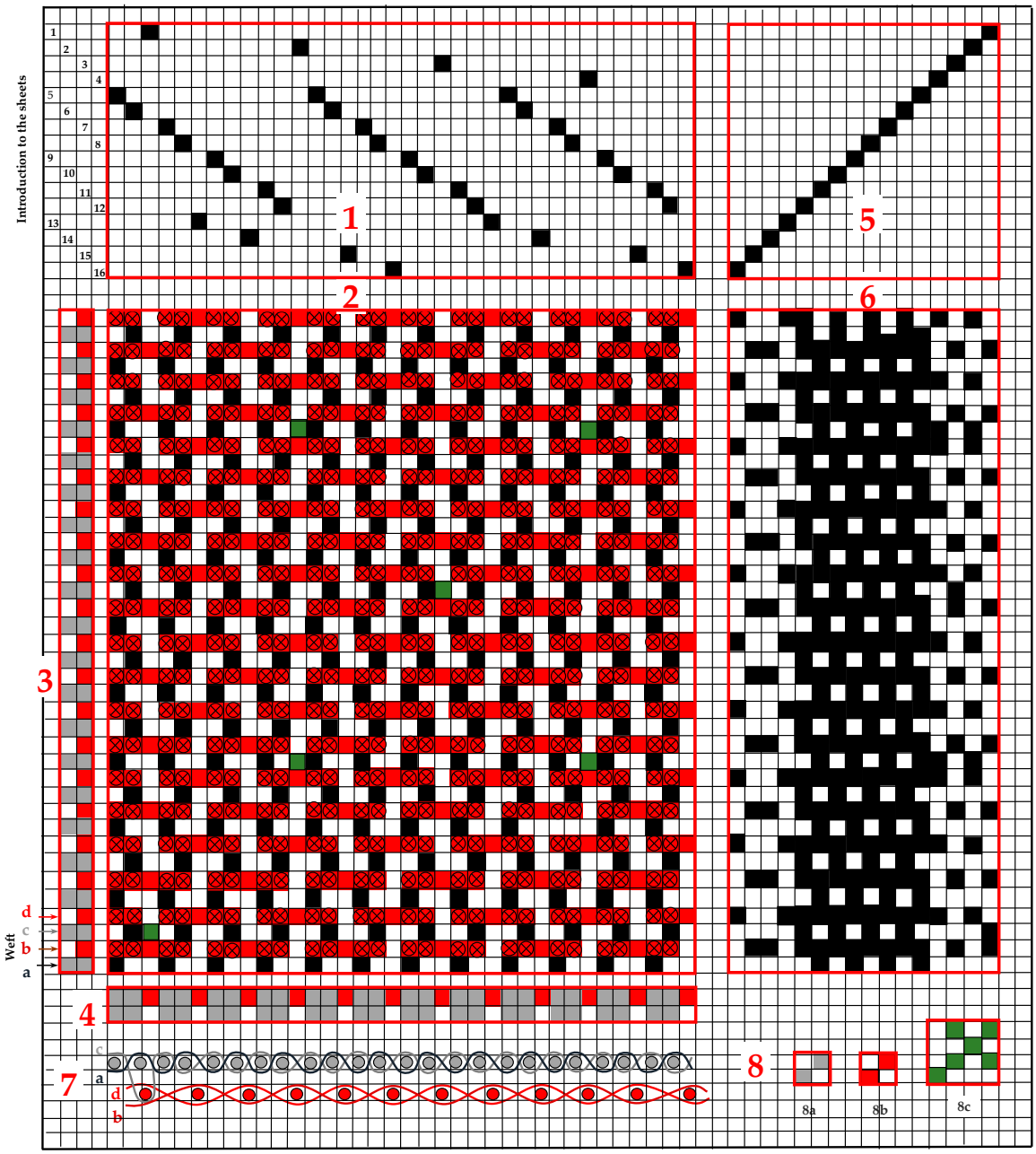

Figure 4. Structural elements and weave of 3D pp fabric. 1—introduction to sheets, 2—unit of weave, 3—order of weft threads, 4—order of warp threads, 5—underweave, 6—map of weave, 7—section of fabric in the weft direction, 8—basic weaves, 8a—weave in the upper fabric; 8b: weave in the lower fabric; 8c—weave for tying the upper and lower fabric; in the unit of weave: —upper fabric, —lower fabric, —interlacing places; —full lifting of the warp threads of the upper fabric when weaving the weft into the lower fabric, numbers 1–16—number of sheet, letters a, b, c, d—order of wefts.

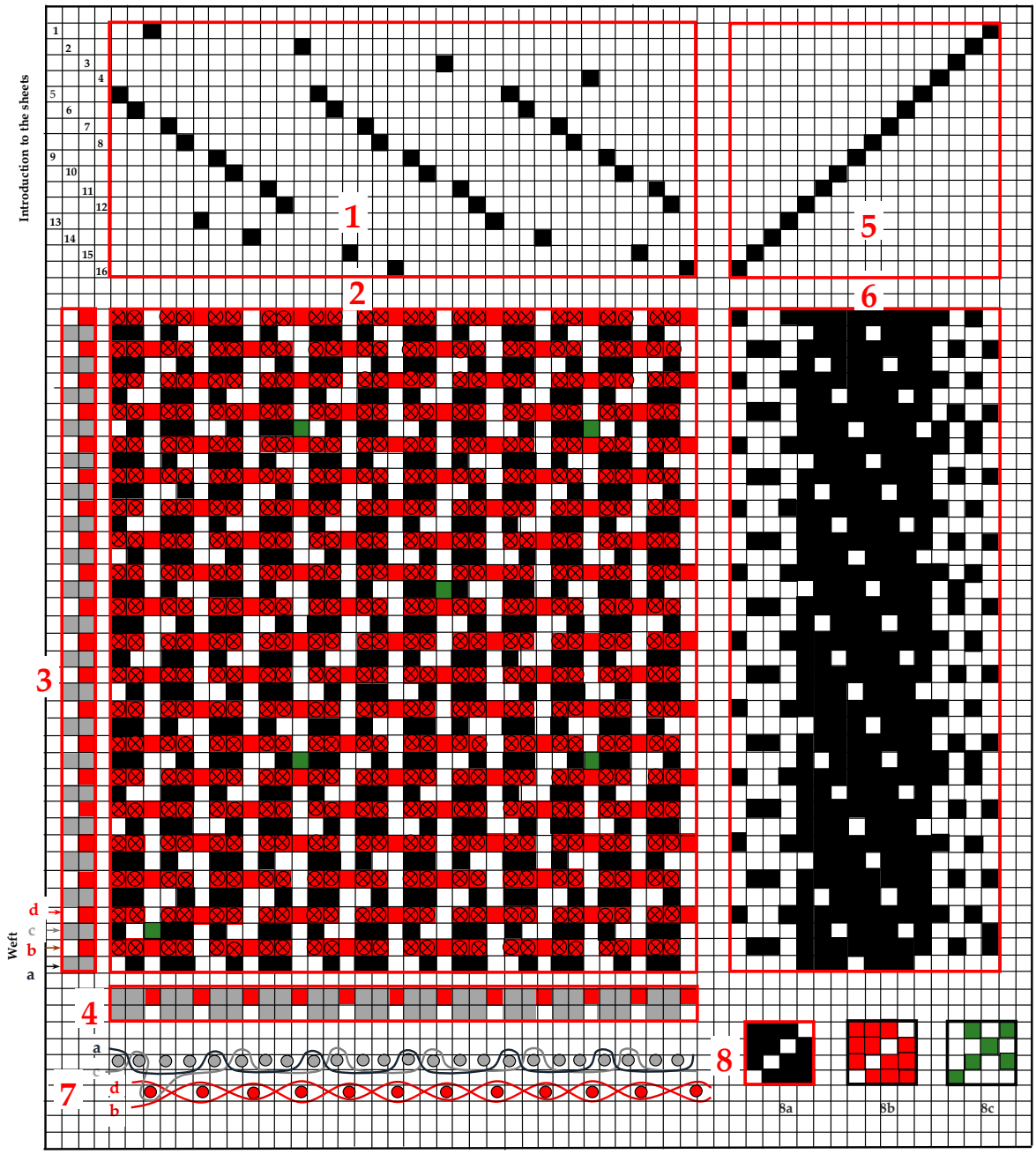

Figure 5. Structural elements and weave of 3D tp fabric. 1—introduction to sheets, 2—unit of weave, 3—order of weft threads, 4—order of warp threads, 5—underweave, 6—map of weave, 7—section of fabric in the weft direction, 8—basic weaves; 8a—weave in the upper fabric; 8b: weave in the lower fabric; 8c—weave for tying the upper and lower fabric; in the unit of weave: —upper fabric, —lower fabric, —interlacing places; —full lifting of the warp threads of the upper fabric when weaving the weft into the lower fabric, numbers 1–16—number of sheet, letters a, b, c, d—order of wefts.

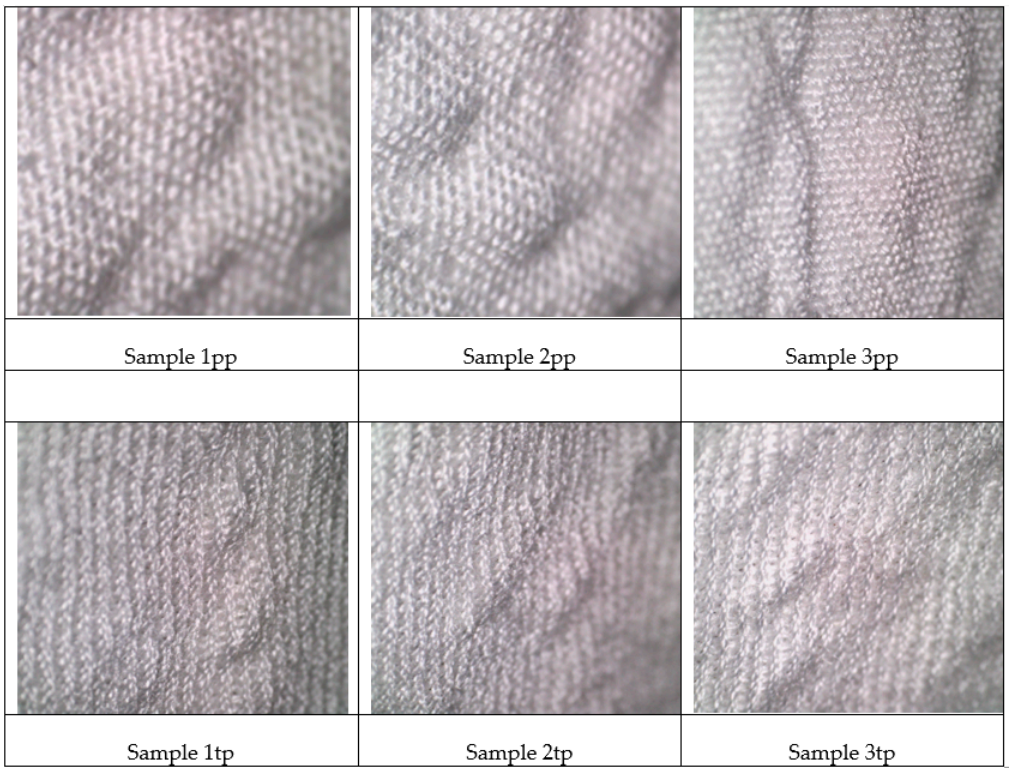

Figure 6. Microscopic image of the surface of 3D-woven fabrics.

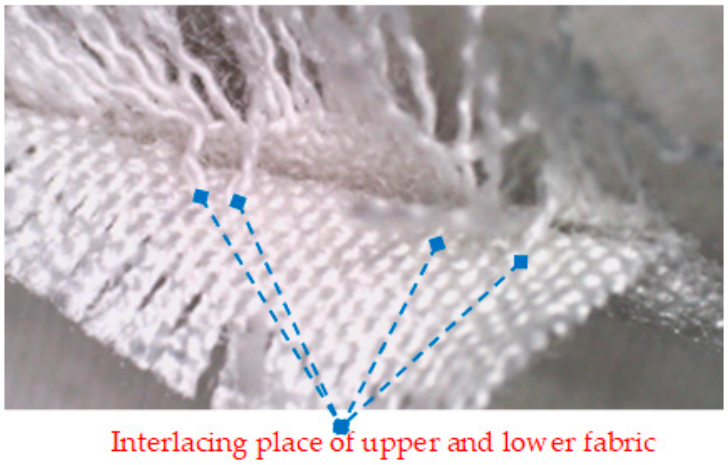

Figure 7. Cross-section of 3D woven fabric marked "1pp" (magnification 20×).

2.3. Methods

2.3.1. Resistance to Radiant Heat According to the Method EN ISO 6942:2022 [21]

The main function of the fabric that protects against high temperatures is to resist the transfer of heat from the thermal environment to the wearer's body in order to protect it from burns. Heat transfer by radiation was tested according to EN ISO 6942:2022 [21] test method B, with the heat flux Q_0: 20 kW/m^2. The test was performed using equipment manufactured according to the regulations of the standard (Figure 8) in the accredited laboratory MIRTA-KONTROL d.o.o. (Croatia) according to the requirements of the standard ISO/IEC 17025:2017 [22].

Figure 8. Laboratory test equipment for determining the resistance to radiant heat according to the method EN ISO 6942 [21].

The equipment consists of a stainless steel frame to protect against direct contact with the heat source, 6 silicon carbide heating rods (1100 °C) with an automatic electronically controlled power compensator due to rod aging and voltage variations mounted on a mobile stand with automatic positioning depending on the required density heat flow, central control unit for automatic calibration from 5 to 80 kW/m^2 and fully automated measuring procedure (time required for temperature rise of 12, 24 and 30 °C), sample holder with a calorimeter and LCD screen with buttons for the management and reading of results.

The density of the transmitted heat flow through the sample is measured using a calorimeter and calculated according to Equation (1):

$$Qc = \frac{\left(M_{bp} \cdot C_p \cdot 12\right)}{A \cdot (t_{24} - t_{12})} = \frac{66.131}{(t_{24} - t_{12})} \quad (1)$$

where

M_{bp} = the mass of the copper plate, which is equal to 0.036 kg.
C_p = the specific heat of copper, which is 0.385 kJ/kg°C.
A = the area of the copper plate, which is equal to 0.002515 m^2.
t_{24} and t_{12} = the time required for the temperature to rise from 12 °C or 24 °C.

The heat transfer factor expresses the heat flow over 1 h that passes through 1 m^2 of fabric of real thickness and a temperature difference of two media of 1 °C. A high TFQ_0 indicates good heat transfer (low thermal stress, i.e., good low-energy comfort under normal operating conditions), while a low heat transfer factor indicates good insulation. The heat transfer factor was calculated according to Equation (2):

$$TFQ_0 = \frac{Q_c}{Q_0} \quad (2)$$

where

Q_C = the density of the transmitted heat flow through the sample to the calorimeter in kW/m^2.
Q_0 = the given heat density (radiation source per calorimeter) in kW/m^2.
TFQ_0 = heat transfer factor.

Three samples of each 3D fabric (dimensions 25 × 8 cm) were tested under the laboratory conditions of a temperature of 20 ± 2 °C and a relative humidity of 65 ± 4%.

2.3.2. Measurement of Thermal and Water-Vapor Resistance EN ISO 11092:2014 [23]

Fabrics with a high degree of protection against high temperatures must have good physiological properties. To determine the physiological properties, we used the EN ISO 11092:2014 method [23], and the tests were carried out on the device according to the regulations of the standard in the accredited laboratory MIRTA-KONTROL d.o.o. (Croatia) according to the requirements of the standard ISO/IEC 17025 [22].

The method determines thermal resistance and water vapor resistance in stationary conditions.

The thermal resistance of the fabric refers to the ratio of the temperature difference on both sides and the heat flow per unit area perpendicular to the fabric (Equation (3)).

$$R_{ct} = \frac{(T_m - T_a) \cdot S}{(H - \Delta H_c)} \quad (3)$$

R_{ct} = thermal resistance of the fabric, $m^2 \cdot K/W$.

The resistance of the fabric to water vapor refers to the ratio of the difference in water vapor pressure on both sides of the fabric and the heat flux evaporated vertically per unit area of the fabric (Equation (4)).

$$R_{et} = \frac{(P_m - P_a) \cdot S}{(H - \Delta H_e)} \quad (4)$$

R_{et} = water vapor resistance, $m^2 \cdot Pa/W$;
T_m = temperature of the metal plate, K;
T_a = temperature of the test area, K;
P_m = pressure of saturated water vapor when the temperature of the metal plate is T_m, Pa;
P_a = water vapor pressure when the temperature of the test chamber is T_a, Pa;
H = heating power of the metal plate, W;
S = surface of the metal plate, m^2;
ΔH_c = heating power correction in thermal resistance testing;
ΔH_e = correction of heating power when testing resistance to water vapor.

The tests were performed under the following conditions: a test plate temperature of 35 °C and air flow speed 1 ± 0.05 m/s.

3. Results

3.1. Test Results According to the Method EN ISO 6942:2022 [21]

The test results according to the EN ISO 6942:2022 [21] method are shown in Table 2.

Table 2. Test results according to EN ISO 6942:2022 [21].

3D Samples		1pp	2pp	3pp	1tp	2tp	3tp
t_{12} (s)	Mean	7.9	7.8	7.9	8.3	8.2	7.6
	CV (%)	1.91	1.59	2.16	1.50	2.08	0.62
t_{24} (s)	Mean	14.3	14.4	14.4	14.9	14.6	13.9
	CV (%)	1.05	1.18	1.13	1.10	1.40	0.59
t_{24}–t_{12} (s)	Mean	6.4	6.6	6.5	6.6	6.4	6.3
	CV (%)	0	0.72	0.72	1.90	0.73	1.30
$RHTI_{24}$–$RHTI_{12}$ (s)	Mean	6.4	6.6	6.5	6.6	6.4	6.3
	CV (%)	0	0.72	0.72	1.90	0.73	1.30
Qc (kW/m^2)	Mean	10.33	10.02	10.17	10.02	10.33	10.50
	CV (%)	0	0.14	0.70	1.90	0.70	1.29
TFQ_0 (-)	Mean	0.5165	0.5010	0.5085	0.5010	0.5165	0.5250
	CV (%)	0	0.14	0.70	1.90	0.70	1.29

From the results in Table 2, it is evident that 3D fabrics 2pp and 1tp provided the highest resistance to radiant heat, where the transmitted heat flow was 10.02 kW/m^2, and the heat transfer factor was 0.5010. It took 7.8 s for the 2pp fabric, and 8.2 s for the 1tp fabric. For the calorimeter temperature to rise to 24 °C, it took 14.4 s for the 2pp fabric and 14.6 s for the 1tp fabric. Fabrics 2pp and 1tp passed the same heat flux density to the calorimeter 10.02 kW/m^2, although the surface mass of fabric 1tp was 6% less (316 g/m^2) than the surface mass of fabric 2pp (336 g/m^2). Sample 3tp provided the lowest resistance to radiant heat; the transmitted heat flux was 10.50 kW/m^2 with a heat transfer factor of 0.5250.

3.2. Test Results According to the Method EN ISO 11092:2014 [23]

The results of testing the thermal resistance of the fabric (Rct) and water vapor resistance (Ret) according to EN ISO 11092:2014 [23] are shown in Table 3.

Table 3. Test results of thermal resistance, Rct, and water vapor resistance, R_{et}.

3D Samples		1pp	2pp	3pp	1tp	2tp	3tp
R_{ct} (m^2·K/W)	Mean	0.0537	0.0501	0.0562	0.0584	0.0576	0.0582
	CV (%)	7.24	4.47	3.70	4.27	6.00	7.28
R_{et} (m^2·Pa/W)	Mean	5.02	5.39	5.11	6.18	5.73	4.95
	CV (%)	3.44	1.47	1.53	1.28	2.94	1.11

Table 3 shows that the water vapor resistance values, Ret, range from 4.94 m^2·Pa/W for fabric 3tp to 6.18 m^2·Pa/W for fabric 1tp. The thermal resistance value (Rct) was the highest for 1tp fabric, 0.0584 m^2·K/W. The lowest thermal resistance of only 0.0501 m^2·K/W belonged to the 2pp fabric.

3.3. The Relationship between the Water Vapor Resistance Value (Ret) and the Surface Mass

The graph in Figure 9 shows the water vapor resistance (Ret) of the 3D fabric and the surface mass. The smallest value of Ret = 4.95 m^2·Pa/W belongs to sample 3pt with the smallest surface mass of 287 g/m^2. It is interesting that the next water vapor resistance value, Ret = 5.02 m^2·Pa/W, belongs to the 1pp sample with the highest surface mass of 356 g/m^2. In general, the diagram shows that samples of 3D fabrics with larger surface masses (1pp, 2pp, 3pp) in which the upper fabric is made of aramid fibers in the fabric and the lower fabric is made of modacrylic fibers in the fabric have lower Ret values, i.e., they provide less water vapor resistance for 3D tp fabrics, which means that they have better thermophysiological properties.

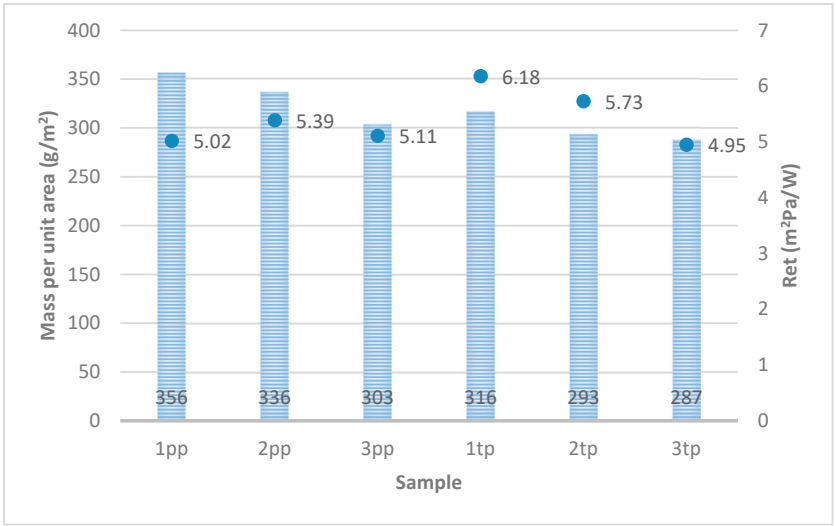

Figure 9. Diagram of resistance of 3D fabrics to water vapor, Ret (m^2·Pa/W).

3.4. The Relationship between the Value of Thermal Resistance (Rct) and the Surface Mass

The graph in Figure 10 shows the thermal resistance values of 3D fabrics and their surface mass. The diagram shows that the sample 2pp has the lowest thermal resistance of 0.0501 $m^2 \cdot K/W$ with a surface mass of 336 g/m^2, and fabric 1tp has the highest value of 0.0584 $m^2 \cdot K/W$ with a surface mass of 316 g/m^2. From the diagram, it can be observed that the samples of 3D fabrics with larger surface masses (1pp, 2pp, 3pp) have lower thermal resistance values, Rct, so the developed metabolic heat passes more easily through the fabric into the atmosphere compared to tp fabrics.

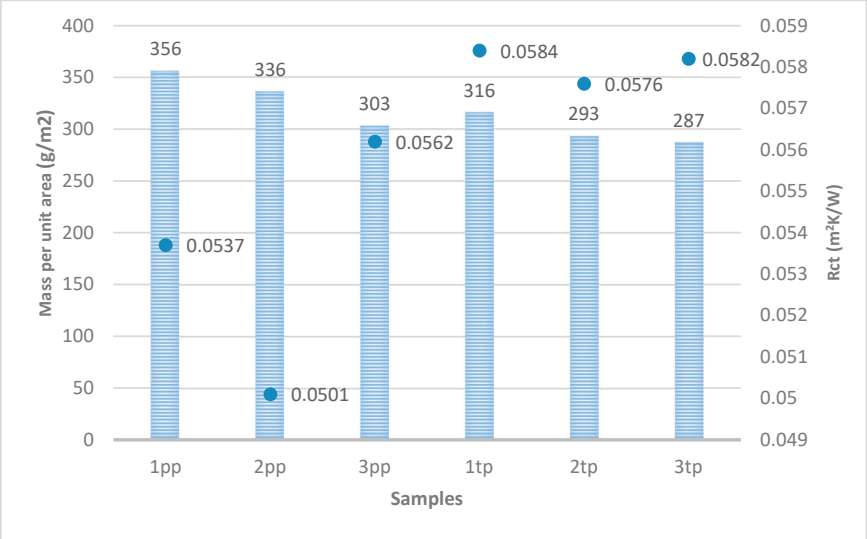

Figure 10. Diagram of thermal resistance of 3D fabrics, R_{ct} ($m^2 \cdot K/W$).

3.5. Relationship between the Density of the Transmitted Heat Flux (Qc) and the Surface Mass

Figure 11 shows the density values of the transmitted heat flux through the sample to the calorimeter in relation to the surface mass. The diagram shows the correlation of fabric tp with surface mass, i.e., by reducing the surface mass of samples 1tp (316 g/m^2)—2tp (293 g/m^2)—3tp (287 g/m^2), the amount of heat flux Qc increases from 10.02 kW/m^2—10.33 kW/m^2—10.50 kW/m^2. The same correlation is not seen with pp 3D fabrics. Fabric 1pp, which has the highest surface mass of 356 g/m^2, has a heat flow of 10.33 kW/m^2. On the other hand, samples 2pp and 3pp with a lower surface mass provide better resistance to radiant heat. Which show us the lower values of the density of the transferred heat flow through the sample to the calorimeter, Qc = 10.02 kW/m^2 and 10.17 kW/m^2.

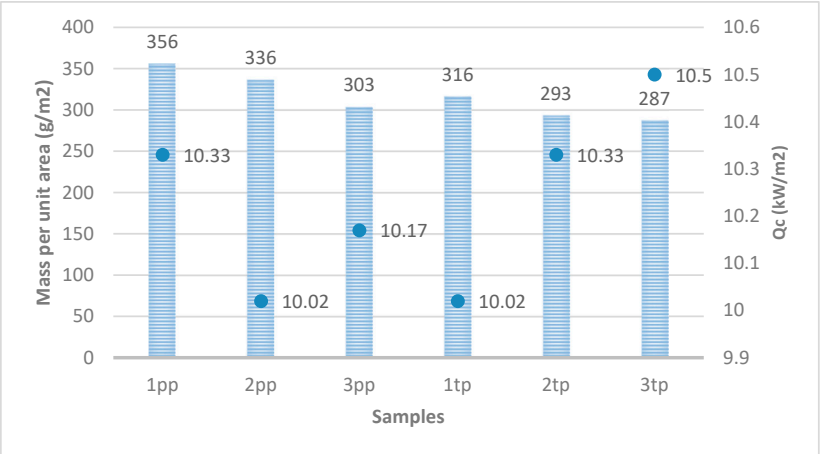

Figure 11. Diagram of the density of the transmitted heat flux of 3D fabrics, Qc (kW/m^2).

3.6. Correlation of the Obtained Qc, Rct and Ret Results with the Weft Density of the Upper Fabric and the Weft Density of the Lower Fabric

Given that the investigated 3D fabrics in this paper consist of a warp, a weft and pre-woven threads of the warp or weft that connect the upper and lower fabric at the connecting points, the correlation of the obtained results Qc, Rct and Ret with the density of the weft is demonstrated in the analysis of the upper and lower fabric weft density.

Based on the data from Table 4, the following conclusions can be made for the 'pp' samples:

1. Correlation of Qc with the weft densities of the upper and lower fabric:
   - Weft density upper fabric—Qc has a moderate positive correlation of 0.6109 with the weft density of the upper fabric. A lower density of the weft leads to a lower density of transmitted heat flow through the sample to the calorimeter. With the reduction in the weft, the resistance to radiant heat increases moderately.
   - Weft density lower fabric—Qc has a low positive correlation of 0.3449 with weft density. A decrease in weft density in the lower fabric causes a lower density of transmitted Qc, leading to a small increase in radiant heat resistance.
2. Correlation of Ret with the weft densities of the upper and lower fabric:
   - Weft density upper fabric—Ret has a low negative correlation of −0.3432 with weft density in the upper fabric, which indicates that the decrease in weft density in the upper fabric has little effect on the increase in Ret, i.e., the resistance to the passage of water vapor increases.
   - Weft density lower fabric—Ret has a negligible correlation of −0.0452 with the weft density of the lower fabric, i.e., the weft density of the lower fabric has a negligible influence on Ret.
3. Correlation of Rct with the weft densities of the upper and lower fabric:
   - Weft density upper fabric—Rct has a low negative correlation of −0.3002 with the weft density of the upper fabric.
   - Weft density lower fabric—the correlation between Rct with the weft density of the lower fabric is moderately negative, i.e., −0.5729. Increasing the density of the weft in the lower fabric leads to a decrease in Rct, i.e., less thermal insulation.

Table 4. Coefficients between pairs of data.

pp Samples	**WDUF**	**WDLF**	**Qc**	**Rct**	**Ret**
Weft density upper fabric (WDUF)	1				
Weft density lower fabric (WDLF)	0.9538	1			
Q_c	0.6109	0.3449	1		
R_{ct}	−0.3002	−0.5729	0.5718	1	
R_{et}	−0.3432	−0.0452	−0.9533	−0.7929	1
tp Samples	**WDUF**	**WDLF**	**Qc**	**Rct**	**Ret**
Weft density upper fabric (WDUF)	1				
Weft density lower fabric (WDLF)	0.9538	1			
Q_c	−0.9987	−0.9370	1		
R_{ct}	0.3500	0.0524	−0.3981	1	
R_{et}	0.9641	0.9993	−0.9491	0.0888	1

Based on the data from Table 4, the following can be observed for the 'tp' samples:

1. Correlation of Qc with the weft densities of the upper and lower fabric:
   - Weft density upper fabric—a strong, negative correlation of 0.9987 Qc with weft density can be observed. By increasing the weft density of the upper fabric, the Qc value decreases. Thus, by increasing the density of the weft, less heat flows through the fabric, i.e., the fabric provides greater resistance to radiant heat.

- Weft density lower fabric—a strong, negative correlation of −0.9370 Qc with weft density of the lower fabric can be observed. By increasing the density of the lower fabric, the density of the transmitted heat flow through the calorimeter, i.e., the Qc value, decreases.

2. Correlation of Ret with the weft densities of the upper and lower fabric:
   - Weft density upper fabric—a strong positive correlation of 0.9641 Ret with the weft density of the upper fabric. A higher density of the weft provides greater resistance to the passage of water vapor. As the density of the weft increases, the comfort of the fabric decreases.
   - Weft density lower fabric—a strong positive correlation 0.9993 Ret with the weft density of the lower fabric can be observed. A higher density of the weft in the lower fabric increases the resistance to the passage of water vapor. As the weft density of the bottom fabric increases, the comfort of the fabric decreases.
3. Correlation of Rct with the weft densities of the upper and lower fabric:
   - Weft density upper fabric—a moderately positive correlation of 0.3500 Rct with weft density can be observed. By increasing the density of the weft, the thermal resistance increases.
   - Weft density lower fabric—there is no correlation between the weft density of the bottom fabric and the Rct.

4. Discussion

If we analyze the diagrams in Figures 9–11, we can notice that the 'pp' samples have better physiological properties and provide better resistance to radiant heat. The diagram in Figure 9 shows that the samples of 3D fabrics with larger surface masses (1pp, 2pp, 3pp), in which the upper fabric is made of aramid fibers in the plain weave and the lower fabric is made of modacrylic fibers also in the plain weave, have lower Ret values, i.e., they provide lower water vapor resistance than 3D tp fabrics, which indicates better thermophysiological properties. Figure 8 also shows that samples of 3D fabrics with larger surface masses (1pp, 2pp, 3pp) have lower Rct values, i.e., lower thermal resistance and good heat transfer, so the developed metabolic heat passes more easily through the fabric into the atmosphere compared to 'tp' fabrics. This is further evidence of the better physiological properties of 'pp' 3D samples. The diagram in Figure 11 shows that with 'tp' fabrics, the amount of heat flow increases with the decrease in surface mass. The same correlation is not seen with 'pp' 3D fabrics, which provide better resistance to radiant heat with smaller surface masses.

In order to further investigate the reason for the behavior of each separate set of 3D samples, 'pp' and 'tp' fabrics, the correlation of the obtained Qc, Rct and Ret results with the weft density of the upper and weft density of the lower fabric was analyzed (Table 4). Based on the obtained correlation factors, we conclude that the increase in the weft density of the upper and lower fabric of the 'tp' samples affects the increase in resistance to radiation heat, but at the expense of physiological properties, and ultimately the 'tp' samples gain higher Ret and Rc values. In the case of 'pp' samples of 3D fabrics, Table 4 shows that by reducing the weft, the resistance to radiation heat increases, but the thermo-physiological properties are not impaired, but are better compared to 'tp' fabrics. Such characteristics are absolutely necessary for fabrics used as fabrics for protection against high temperatures.

The upper fabric, which forms the face of the higher density aramid fiber fabric, has a uniform surface. The lower fabric, made of cotton and modacrylic, has a lower density and a wrinkled surface created by interweaving with the upper fabric. The surface folds of the fabric, which were created by weaving, create pockets filled with air (volumetric porosity) between the fabrics. The increase in the weft density leads to more dense and more frequent folds, and decreases the air volume in the pockets. This process has an effect on the volume, thickness and weight of the fabric. The folds of pp fabrics are more noticable when applied to tp samples. The folds show actual trapped air in the pore pockets of the fabric, which serve as a heat insulator, thus increasing the protection against the thermal

radiation. If we observe the pp samples, sample 2pp gave the best results of thermal resistance to radiation (Qc = 10.02 m^2·K/W) and the lowest value of thermal resistance (Rct = 0.0502). The water vapor resistance value of the 1pp sample with the highest density and surface mass, Ret = 5.02 mPa/W, is just behind the 3tp sample with the lowest surface mass. The described structure of the sample is responsible for these results. The trapped air in the pockets of fabric pores provides greater resistance to radiant heat [14]. The resulting folds also give the fabric better physiological properties and better breathability, which means that the developed metabolic heat is more easily released into the environment. The binding yarn intertwines from one fabric to another, and its tension creates larger pores in pp samples where the upper fabric is in the plain weave. Microscopic analysis (Figure 6) showed that the folds of tp fabrics are not as apparent as those of pp fabrics. Given that in tp fabric, the upper fabric in twill is a 3/1 weave, there is less tension in the binding yarn that intertwines from one fabric to another. As a result, folds are not formed as with the pp samples [20]. The results of Qc, Rct and Ret values of fabric tp are in accordance with this. By increasing the density of the upper and lower fabric, the surface mass increases. Therefore, sample 1tp provides the best resistance to thermal radiation, but its physiological properties Rct and Ret are the worst. Sample 3tp demonstrated the worst resistance to radiant heat, while its physiological properties were good. All of the above is supported by the presented correlation coefficients for tp samples, looking at each fabric (upper and lower) as a separate segment.

The wrinkled surface structure of 'pp' 3D fabrics allows fabrics with the described structure to be an alternative to single-layer fabrics and composites present on the market for thermal protective clothing. Compared to the fabrics used today, the newly developed three-dimensional fabrics have improved properties in the domain of thermophysiological comfort and improved thermal protection (creating an air space in the cross-section of the fabric as a heat insulator) against extreme temperatures.

5. Conclusions

According to the results obtained, the following can be concluded:

- The 'pp' samples of 3D fabrics with larger surface masses, where the upper fabric is made of aramid fibers in the fabric and the lower fabric is made of modacrylic fibers also in the fabric, have lower Ret values, i.e., they provide less resistance to the passage of water vapor than 3D' tp' fabric.
- The 'pp' samples of 3D fabrics with larger surface masses have lower Rct values, i.e., lower thermal resistance, thus good heat transfer, so the developed metabolic heat passes more easily through the fabric into the atmosphere compared to 'tp' fabrics.
- The amount of transmitted heat flux 'tp' of fabrics increases with the reduction in the surface mass. The same correlation is not observed with 'pp' fabrics, which provide better resistance to radiant heat with smaller surface masses.
- Increasing the weft density of the upper and lower fabric of 'tp' fabric affects the increase in resistance to radiant heat, but to the detriment of physiological properties.
- In the case of 'pp' samples, by reducing the weft, the resistance to radiation heat increases, but the thermo-physiological properties are not impaired.
- The 'pp' samples provide better thermophysiological properties and better resistance to radiant heat compared to 'tp' fabrics.
- The reason for the better results in terms of thermophysiological properties and resistance to radiant heat is in the structure of 'pp' fabrics compared to 'tp' fabrics.
- The folds present in "pp" fabrics are less frequent with a larger volume of "trapped" air in the "pockets" that create the fabric pores, which gives greater resistance to radiation heat-lines and better physiological properties.
- By increasing the weft density, the folds present in 'tp' fabrics are denser and more frequent, with a smaller volume of air, which affects the volume, thickness and mass of the fabric, and therefore 'tp' fabrics have worse thermophysiological properties and offer less resistance to radiant heat compared to 'pp' fabrics.

Author Contributions: Conceptualization, A.K. and S.K.; methodology, A.K. and S.K.; software, A.K. and S.K.; validation, A.K.; formal analysis, A.K. and S.K.; investigation, A.K. and S.K.; resources, S.K.; data curation, A.K. and S.K.; writing—original draft preparation, A.K. and S.K.; writing—review and editing, A.K. and S.K.; visualization, A.K. and S.K.; supervision, S.K.; project administration, S.K.; funding acquisition, S.K. All authors have read and agreed to the published version of the manuscript.

Funding: This research received no external funding.

Data Availability Statement: Data are contained within the article. The raw data supporting the conclusions of this article will be made available by the authors on request.

Acknowledgments: We express our sincere gratitude to all associates from the University of Zagreb Faculty of Textile Technology, Zagreb, Croatia.

Conflicts of Interest: The author Ana Kiš is employed by the company Vertiv Croatia. The remaining authors declare that the research was conducted in the absence of any commercial or financial relationships that could be construed as a potential conflict of interest.

References

1. Kahn, S.A.; Patel, J.H.; Lentz, C.W. Firefighter burn injuries: Predictable patterns influenced by turnout gear. *J. Burn Care Res.* **2012**, *33*, 152–156. [CrossRef] [PubMed]
2. Song, G.; Mandal, S.; Rossi, R. *Thermal Protective Clothing for Firefighters*; Woodhead Publishing: Kidlington, UK, 2016; ISBN 978-0081012857.
3. Song, G.; Paskaluk, S.; Sati, R. Thermal protective performance of protective clothing used for low radiant heat protection. *Text. Res. J.* **2011**, *81*, 311–323. [CrossRef]
4. Lei, Z. Review of the study of relation between the thermal protection performance and the thermal comfort performance of firefighters' clothing. *J. Eng. Fibers Fabr.* **2022**, *17*, 1–9. [CrossRef]
5. Barker, R. Evaluating the heat stress and comfort of firefighter and emergency responder protective clothing. In *Improving Comfort in Clothing*; Woodhead Publishing: Kidlington, UK, 2011; pp. 305–319, Chapter 12, ISBN 9781845695392.
6. Choudhury, A.K.R.; Majumdar, P.K.; Datta, C. Factors affecting comfort: Human physiology and the role of clothing. In *Improving Comfort in Clothing*; Woodhead Publishing: Kidlington, UK, 2011; pp. 3–60, Chapter 1, ISBN 9781845695392.
7. Asif, M.; Kala, C.; Gilani, S.J.; Imam, S.S.; Taleuzzaman, M.; Alshehri, S.; Khan, N.A. Protective clothing for firefighters and rescue workers. In *Protective Textiles from Natural Resources*; Volume in The Textile Institute Book Series; Woodhead Publishing: Sawston, UK, 2022; pp. 611–647.
8. Lawson, L.K.; Crown, E.M.; Ackerman, M.Y.; Douglas Dale, J. Moisture effects in heat transfer through clothing systems for wildland firefighters. *Int. J. Occup. Saf. Ergon.* **2004**, *10*, 227–238. [CrossRef] [PubMed]
9. Limeneh, D.Y.; Ayele, M.; Tesfaye, T.; Liyew, E.Z.; Tesema, A.F. Effect of Weave Structure on Comfort Property of Fabric. *J. Nat. Fibers* **2020**, *18*, 8. [CrossRef]
10. Frydrych, I.; Dziworska, G.; Bilska, J. Comparative analysis of the thermal insulation properties of fabrics made of natural and manmade cellulose fibres. *Fibers Text. East. Eur.* **2002**, *10*, 40–44.
11. Abdel-Rehim, Z.S.; Saad, M.M.; El-Shakankery, M.; Hanafy, I. Textile fabrics as thermal insulators. *Autex Res. J.* **2006**, *6*, 148–161. [CrossRef]
12. Ahmad, S.; Ahmad, F.; Afzal, A.; Rasheed, A.; Mohsin, M.; Ahmad, N. Effect of weave structure on thermo-physiological properties of cotton fabrics. *Autex Res. J.* **2015**, *15*, 30–32. [CrossRef]
13. Kovačević, S.; Schwarz, I.; Brnada, S. *Technical Fabrics*; University of Zagreb, Faculty of Textile Technology: Zagreb, Croatia, 2019; ISBN 978-953-7105-78-5.
14. Kiš, A.; Brnada, S.; Kovačević, S. Influence of Fabric Weave on Thermal Radiation Resistance and Water Vapor Permeability. *Polymers* **2020**, *12*, 525. [CrossRef] [PubMed]
15. Bilisk, K. New method of weaving multiaxis three dimensional flat woven fabric: Feasibility of prototype tube carrier weaving. *Fibres Text. East. Eur.* **2009**, *17*, 63–69.
16. Bilisik, K. Multiaxis three dimensional (3D) woven fabric. In *Advances in Modern Woven Fabrics Technology*; IntechOpen: London, UK, 2011.
17. Ansar, M.; Xinwei, W.; Chouwei, Z. Modeling strategies of 3D woven composites: A review. *Compos. Struct.* **2011**, *93*, 1947–1963. [CrossRef]
18. Zahid, B.; Chen, X. Manufacturing of single-piece textile reinforced riot helmet shell from vacuum bagging. *J. Compos. Mater.* **2013**, *47*, 2343–2351. [CrossRef]
19. El-Dessouky, H.M.; Snape, A.E.; Turner, J.L.; Saleh, M.N.; Tew, H.; Scaife, R.J. 3D weaving for advanced composite manufacturing: From research to reality. In Proceedings of the SAMPE Conference, Seattle, DC, USA, 22–25 May 2017.
20. Kovačević, S.; Rogina-Car, B.; Kiš, A. Application of 3D-Woven Fabrics for Packaging Materials for Terminally Sterilized Medical Devices. *Polymers* **2022**, *14*, 4952. [CrossRef] [PubMed]

21. *EN ISO 6942:2022*; Protective Clothing—Protection against Heat and Fire—Method of Test: Evaluation of Materials and Material Assemblies When Exposed to a Source of Radiant heat. International Organization for Standardization: Geneva, Switzerland, 2022.
22. *ISO/IEC 17025:2017*; General Requirements for the Competencs of Testing and Alibration Laboratories. International Organization for Standardization: Geneva, Switzerland, 2017.
23. *EN ISO 11092:2014*; Textiles—Physiological Effects—Measurement of Thermal and Water-vapour Resistance under Steady-State Conditions (Sweating Guarded-Hotplate Test). International Organization for Standardization: Geneva, Switzerland, 2014.